Resilient Structures and Sustainable Construction
Edited by Pellicer, E., Adam, J. M., Yepes, V., Singh, A., and Yazdani, S.

ISBN: 978-0-9960437-4-8

WIND LOAD PREDICTION OF LARGE-SPAN DRY COAL SHEDS BASED ON GRNN AND ITS APPLICATION

YING SUN[1], LIN YANG[2], and YUE WU[1]

[1]*Key Lab of Structures Dynamic Behavior and Control of the Ministry of Education, School of Civil Engineering, Harbin Institute of Technology, Harbin, China*
[2]*School of Civil Engineering, Harbin Institute of Technology, Harbin, China*

The distribution and fluctuation of wind load on large-span dry coal sheds are complicated. Wind load on typical shape of roofs can be sometimes determined based on the wind tunnel tests carried out on roofs of similar shape. To expand the application scope of the test data, Generalized Regression Neural Network (GRNN) is introduced. The prediction models on large-span dry coal are given, where the wind load is expressed by eight parameters: mean, RMS, skewness, kurtosis of wind pressure coefficients, three auto-spectral parameters (including descendent slope in high frequency range, peak reduced spectrum and reduced peak frequency) and coherence exponent for cross-spectra. Cross validation and trails are carried out to determine the parameter in the GRNN model. Further, the wind load prediction is applied on a dry coal shed shell. The wind-induced responses are calculated and compared with the results of wind tunnel tests, with extremely close result. Therefore, it can be concluded that GRNN is feasible in predicting wind load on roof structures.

Keywords: Neural network, Wind-induced responses, Prediction model.

1 INTRODUCTION

The determination of wind load on large-span roofs is a key problem to wind resistant design of structures. It is suggested that in the Loading Code for the Design of Building Structures (GB50009-2012) that the wind load on important and complex building constructions, should be determined by wind tunnel tests. The development of computer networks and database technology also offers a new platform for wind resistant design of structures in recent years. It can synthesize and systemize existing data, which has not only the full advantage of existing data to avoid repeating wind tunnel test, but also improve the efficiency and accuracy of wind resistant design of structures (Pierre and Kopp 2005, Zhou *et al.* 2003).

The wind loading information stored in database can be generalized and extended via intelligence algorithm, i.e. neural network. Uematsu and Tsuruishi (2008) predicted the wind load statistics on large-span domes via cascade artificial neural network based on the data of wind tunnel tests. Chen *et al*. (2003a) predicted the mean and fluctuating wind pressure on low-rise pitched roof using artificial neural network based on American NIST low-rise buildings. Chen *et al*. (2003b) also predicted other wind load statistics and obtained wind pressure time histories via artificial neural network based on original data stored in database to make structural design more convenient. Fu *et al.* (2003) predicted the distribution of wind pressure on large-span roofs using fuzzy neural network while they haven't lucubrated wind load frequency spectrum.

When building a neural network prediction model, the expression form of wind load should be the first thing to be decided. Usually, the wind load statistics (mean, RMS, skewness, kurtosis of wind pressure coefficients) and simplified wind pressure spectrum model are used. Abundant frequency-domain information is contained in the spectral model of wind loading, which would have significant influence on the dynamic response of structures.

In this paper, the authors use statistics and spectrum parameter to express wind load and further build a wind load prediction model via generalized regression neural network considering the background of wind load database assistant design. In the application of practical projects, wind load time history is generated based on we wind load statistics and spectrum-domain information via stochastic simulation technique and the wind-induced response of structures are obtained. A practical three-column latticed shell is used to verify the validity of this method.

2 GENERALIZED REGRESSION NEURAL NETWORK

Generalized Regression Neural Network (GRNN) is a branch of radial basis function neural network (RBF) which can adjust the network based on the data get from sampling and calculating without the need of recalculate the network parameter. Different from typical back propagation neural network (BP), GRNN can get better simulation result with high efficiency and stability. GRNN is composed by four layers, as shown in Figure 1. They are: Input Layer, Pattern Layer, Summation Layer and Output Layer. Supposing that the input of the network is X = {x1, x2, …, xn}T, and the output is Y = {y1, y2,…ym} T.

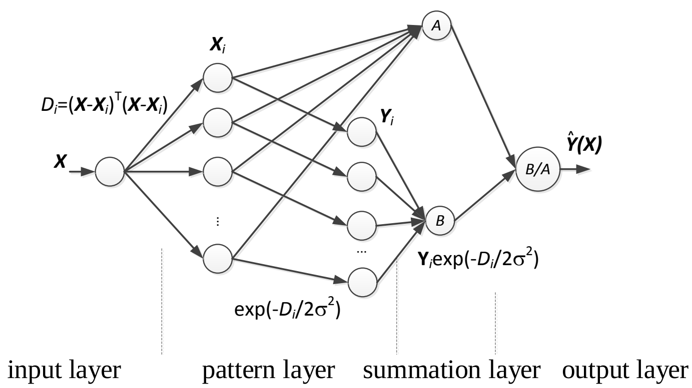

Figure 1. Structure of generalized regression neural network.

The output of GRNN can be estimate by Eq. (1):

$$\hat{Y}(X)=\frac{\sum_i Y_i \exp\left(-\frac{D_i}{2\sigma^2}\right)}{\sum_i \exp\left(-\frac{D_i}{2\sigma^2}\right)} \tag{1}$$

where $\hat{Y}(X)$ is the estimated value of sample which is the weighted mean result of each observed value of the sample Y_i. $D_i=(X-X_i)^{\mathrm{T}}(X-X_i)$ is the weight factor of each observed value Y_i

which is also the exponent of the square value of X_i and X 's Euclidean distance. s is smoothing factor, it can be obtained by trial computation.

3 PREDICTION MODEL OF WIND LOAD ON LARGE-SPAN THREE-COLUMN LATTICED SHELL

3.1 Wind Tunnel Tests of Typical Three-Column Latticed Shell

A series of wind tunnel tests of large-span three-column latticed shells were carried out in the wind tunnel laboratory in Harbin Institute of Technology. The laboratory is 4m wide, 3m high and 25m long. The schematic diagram of the test model is shown as Figure 2. The span of the model is 54cm and the length-width ratio are 1, 1.5, and 2. There are 300 measurement points on the surface of the model. The test wind speed is 10m/s. The sampling frequency is 625Hz and the sample length is 12500. All the pressure fluctuation signal of each test point has been modified.

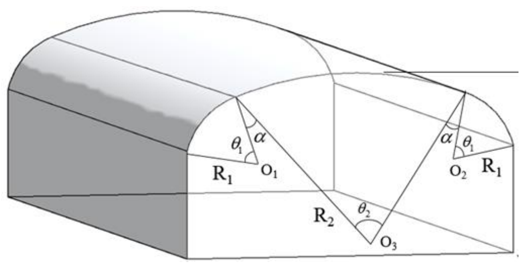

Figure 2. Wind tunnel models.

3.2 Wind Loading Modeling

The inflow dynamic pressures $\frac{1}{2} r U_H^2$ of the wind load at the height of roof H is defined as coefficient of wind pressure C_p after applying dimensionless method. Statistical compute the time-histories of the coefficient of wind pressure, we can get the mean value C_{pmean} , root-mean-square value C_{pRMS} , skewness S_k and kurtosis K_u as the statistics of wind pressure coefficients. The expressions are as follows, Eq. (2) to (5):

$$C_{pmean} = \frac{1}{N} \sum_{i=1}^{N} C_p(t_i) \tag{2}$$

$$C_{pRMS} = \sqrt{\frac{1}{N} \sum_{i=1}^{N} [C_p(t_i) - C_{pmean}]^2} \tag{3}$$

$$S_k = \frac{1}{N} \sum_{i=1}^{N} [\frac{C_p(t_i) - C_{pmean}}{C_{pRMS}}]^3 \tag{4}$$

$$K_u = \frac{1}{N} \sum_{i=1}^{N} [\frac{C_p(t_i) - C_{pmean}}{C_{pRMS}}]^4 \tag{5}$$

where N is the sampling time, t_i is the moment of sample point i.

As for the auto-power spectrum, we use the Three-parameter spectral model (Su Ning, 2014). The equation is, Eq. (6) and (7):

$$\frac{f\cdot S_{Cp}(f)}{C_{pRMS}^2} = S_m \cdot F' \cdot \left(\frac{1-k_2}{F' - k_2}\right)^{\frac{1-k_2}{\alpha}} \tag{6}$$

$$F' = \frac{f\cdot L}{F_m \cdot U_H} \tag{7}$$

where $S_{Cp}(f)$ is auto-power spectrum, F' is dimensionless frequency, k_2, S_m, F_m are three parameters of the auto-power spectrum that represent the decay slope of dimensionless auto-power spectrum at high-frequency section, spectrum peak and dimensionless peak frequency respectively as shown in Figure 3, α is undetermined parameter which can be obtained via k_2 and S_m by Eq.(8). $B(x,y) = \int_0^1 u^{x-1}(1-u)^{y-1}\,\mathrm{d}u$ is Beta function as shown in Eq. (9).

$$S_m \cdot \frac{1}{\alpha} \cdot \left(1 - \frac{1}{k_2}\right)^{\frac{1-k_2}{\alpha}} \cdot \left(-k_2\right)^{\frac{1}{\alpha}} \cdot B\left(\frac{1}{\alpha}, \frac{-k_2}{\alpha}\right) = 1 \tag{8}$$

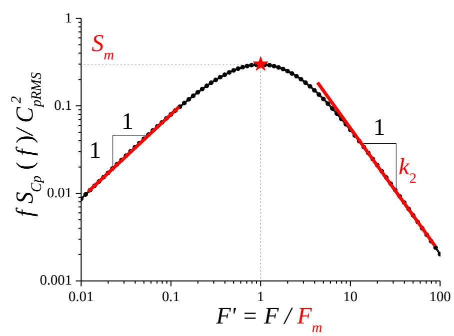

Figure 3. A typical spectral curve and three-parameter auto-spectral model.

The cross-power spectrum $S_{Cpij}(f)$ is coherence function of index type, the expression is:

$$S_{Cpij}(f) = \sqrt{S_{Cpi}(f)\cdot S_{Cpj}(f)}\cdot \exp\left(-k_c \frac{f\cdot \Delta_{ij}}{U_H}\right) \tag{9}$$

where $S_{Cpi}(f)$, $S_{Cpi}(f)$ is the wind load auto-power spectrum of point i and j. k_c is correlation index that can describe the correlation of the fluctuating wind-pressure coefficient of two points in frequency domain. The bigger the value is, the smaller the degree of correlation is. Δ_{ij} is the distance between the two points.

In conclusion, the wind load on the roof can be represented by eight parameters: $\{C_{pmean}, C_{pRMS}, S_k, K_u, k_2, S_m, F_m, k_c\}$.

3.3 Wind Load Prediction Model

According to the wind tunnel test model, select the rise-span ratio *r/L*, depth-span ratio *h/L*, wind angle, open form and x, y, z coordinate as the input training data and each element of wind load description vector as output data for neural network. Because of the difference of rise-span ratio and depth-span ratio of the test model, the total data group is 3255. Divide the data into training set and prediction set on the basis of working condition for the neural network training. Use error exponent I_E and correlation coefficient R to evaluate the prediction outcome. The expressions are, Eq. (10) and (11):

$$I_E = \frac{\sqrt{\frac{1}{M}\sum_{k=1}^{M}\left(T_k - O_k\right)^2}}{\sigma_0} \tag{10}$$

$$R = \frac{\sum_{k=1}^{M}(T_k - \bar{T})\cdot(O_k - \bar{O})}{\sqrt{\sum_{k=1}^{M}(T_k - \bar{T})^2 \cdot \sum_{k=1}^{M}(O_k - \bar{O})^2}} \tag{11}$$

where T_k is the prediction value and O_k is the target value, M is the sample size and σ_0 is the standard deviation of the sample value; $\bar{T}$ and $\bar{O}$ are the mean value of prediction and target value. The smaller I_E is and the closer R to 1 is, the more efficient the prediction.

Figure 4 shows the influence of different smoothing factor σ to mean and fluctuating wind pressure of prediction. We see that different σ values have great influence on the predicted outcome, and according to the training outcome, we choose 0.2 as the smoothing factor.

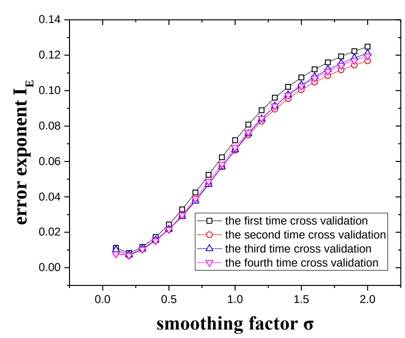

Figure 4. Influence of smooth factor σ on the prediction.

Figure 5 shows the training outcome using cross validation of the closed roof of rise-span ratio 0.37, length-span ratio 1/1.5 and wind angle 60. Table 2 shows the evaluation index of each prediction parameter. We can see from Figure 5 and Table 2 that the prediction result of each parameter's over trend of distribution is good even though there is some error in some local value. The prediction result of parameter S_k and K_u is worse than other parameters which is the same as the result of Uematsu and Tsuruishi (2008). However, Uematsu and Tsuruishi (2008) also shows that S_k and K_u describe the non-Gaussian feature of wind pressure coefficient and the fluctuation of calculation outcome of those that are not insensitive to wind-resistant design.

Prediction outcome Test outcome

(a) Mean wind pressure C_{pmean}.

Prediction outcome Test outcome

(b) Fluctuating wind pressure C_{pRMS}.

Figure 5. Comparisons of prediction and test values.

Table 2. Evaluation indexes of wind load prediction based on GRNN.

parameter	C_{pmean}	C_{pRMS}	S_k	K_u	k_2	S_m	F_m	k_c
I_E	0.189	0.593	0.435	0.917	0.574	0.884	0.582	0.484
R	0.983	0.804	0.912	0.398	0.836	0.756	0.825	0.940

4 CONCLUSIONS

(1) The description of fluctuating wind load should contain win load statistics and frequency-spectrum model. This paper use eight characteristic parameters including mean, RMS, skewness, kurtosis of wind pressure coefficients, three auto-spectral parameters (including descendent slope in high frequency range, peak reduced spectrum and reduced peak frequency) and coherence exponent and they can comprehensively reflect the character of fluctuating wind load on structures.

(2) GRNN is preferable in nonlinear fitting and prediction. According to the outcome of this paper, the suggested smoothing factor is from 0 to 2 and the recommend value is 0.5 when predict the mean wind load.

Acknowledgments

This study was financially supported by the National Natural Science Foundation of China under Grant No. 51478155 and 51378147.

References

Chen, Y., Kopp, G. A., Surry, D., Interpolation of Pressure Time Series in an Aerodynamic Database for Low Buildings, *Journal of Wind Engineering and Industrial Aerodynamics*, 91(6): 737 – 765, 2003a.

Chen, Y., Kopp, G. A., Surry, D., Prediction of Pressure Coefficients on Roofs of Low Buildings Using Artificial Neural Networks[J], *Journal of Wind Engineering and Industrial Aerodynamics*, 91(3): 423–441, 2003b.

Fu, J. Y., Xie, Z. N., Ni, Z. H., Prediction of Wind Load on Large Span Roof Using Fuzzy Neuro Networks[J], *Journal of Building Structures*, 23(01): 62-67 (in Chinese), 2002.

GB50009-2012, *Loading Code for the Design of Building Structures*, 2012.

Pierre, L. M., Kopp, G. A., Surry, D., Ho, T., The UWO Contribution to the NIST Aerodynamic Database for Wind Loads on Low Buildings: Part 2. Comparison of Data with Wind Load Provision, *Journal of Wind Engineering and Industrial Aerodynamics*, 93(1) 31–59, 2005.

Uematsu, Y. and Tsuruishi, R., Wind Load Evaluation System for the Design of Roof Cladding of Spherical Domes, *Journal of Wind Engineering and Industrial Aerodynamics*, 96(10-11): 2054-2066, 2008.

Zhou, Y., Kijewski, T., and Kareem, A., Aerodynamic Loads on Tall buildings: An Interactive Database, *Journal of Structural Engineering*, 129(3): 394-404, 2003.